Proteome-wide mapping of cholesterol-interacting proteins in mammalian cells

Jonathan J Hulce, Armand B Cognetta, Micah J Niphakis, Sarah E Tully & Benjamin F Cravatt

Cholesterol is an essential structural component of cellular membranes and serves as a precursor for several classes of signaling molecules. Cholesterol exerts its effects and is, itself, regulated in large part by engagement in specific interactions with proteins. The full complement of sterol-binding proteins that exist in mammalian cells, however, remains unknown. Here we describe a chemoproteomic strategy that uses clickable, photoreactive sterol probes in combination with quantitative mass spectrometry to globally map cholesterol-protein interactions directly in living cells. We identified over 250 cholesterol-binding proteins, including receptors, channels and enzymes involved in many established and previously unreported interactions. Prominent among the newly identified interacting proteins were enzymes that regulate sugars, glycerolipids and cholesterol itself as well as proteins involved in vesicular transport and protein glycosylation and degradation, pointing to key nodes in biochemical pathways that may couple sterol concentrations to the control of other metabolites and protein localization and modification.

The membrane bilayer serves as a physical barrier that defines the outer boundary of cells and segregates their interior into distinct compartments that perform specialized functions. Among the many lipid constituents of mammalian cell membranes, cholesterol is special in that it is a major regulator of membrane fluidity and contributes to the formation of specific membrane structures such as caveolae and other lipid microdomains[1]. Beyond its role in membrane structure, cholesterol also serves as a metabolic precursor for a diverse array of signaling molecules, including oxysterols[2], steroids[3] and bile acids[4]. Deregulation of cholesterol uptake and metabolism is the basis for a range of human diseases that include cardiovascular disorders[5], skin[6] and developmental[7,8] defects, syndromes resulting from defective lysosomal storage[9,10] and neurodegeneration[10,11].

Cholesterol's central role in mammalian physiology mandates that the concentrations of this lipid are tightly regulated in cells. Meeting this objective poses an unusual challenge for cells because the vast majority of cholesterol is embedded in the lipid bilayer. Multiple sterol-sensing pathways have been identified that communicate alterations in the membrane concentrations of cholesterol to the transcriptional and post-transcriptional control of sterol biosynthetic, uptake and transport pathways[12–14]. Beyond these primary control points, cholesterol has also been found to interact with other proteins by both covalent[15] and non-covalent mechanisms[16,17]. These cholesterol-protein interactions are thought to regulate protein stability, localization and activity.

Despite the tremendous progress that has been made in characterizing specific cholesterol-protein interactions, our understanding of the full spectrum of proteins that regulate, and are regulated by, cholesterol remains incomplete, in large part owing to a lack of global methods for mapping proteins that physically interact with sterols in living cells. The biochemical assessment of cholesterol-protein interactions has, to date, been restricted to a limited canon of assays that include direct *in vitro* binding using radiolabeled cholesterol and purified proteins[18] and modification of proteins with radiolabeled photoreactive cholesterol analogs[19,20]. Although these methods have been used to successfully characterize individual protein-cholesterol interactions, the approaches also lack key features, most notably a means for affinity enrichment, that have precluded their incorporation into chemoproteomic platforms for the global discovery of sterol-binding proteins in mammalian cells.

Here we expand the repertoire of available methods for mapping sterol-binding proteins by introducing a chemoproteomic approach to label, enrich and identify cholesterol-interacting proteins from living cells. We applied this approach to identify more than 250 cholesterol-binding proteins in HeLa cells, including several proteins that are known to biosynthesize, transport and regulate cholesterol, as well as many proteins for which no prior interaction with cholesterol has been described.

RESULTS

Design of clickable, photoreactive sterol probes

We reasoned that chemoproteomic probes for mapping cholesterol-binding proteins in living cells would need to have three general features: (i) a photoreactive group for ultraviolet (UV) light–induced cross-linking to probe-interacting proteins, (ii) a latent affinity handle, such as an alkyne group for conjugation to azide-reporter tags by copper-catalyzed azide-alkyne

The Skaggs Institute for Chemical Biology and Department of Chemical Physiology, The Scripps Research Institute, La Jolla, California, USA. Correspondence should be addressed to B.F.C. (cravatt@scripps.edu).

RECEIVED 1 NOVEMBER 2012; ACCEPTED 7 JANUARY 2013; PUBLISHED ONLINE 10 FEBRUARY 2013; DOI:10.1038/NMETH.2368

cycloaddition (CuAAC or click) chemistry[21], which enables detection, enrichment and identification of probe-interacting proteins[22], and (iii) an intact cholesterol scaffold, such that after integration of photo-cross-linking and 'clickable' groups, the resulting probe could still interact with most cholesterol-binding proteins. With these considerations in mind, we designed and synthesized a set of sterol probes (**Fig. 1a**), each of which contains a photoactivatable diazirine group at the 6 position of the steroid core (using standard numbering), which is a modification that previously has been shown to minimally perturb the biophysical properties of cholesterol[23]. The probes also have an alkyne incorporated into the alkyl side chain of cholesterol via an ester linkage, which we chose for ease of synthesis. Although this ester linkage would be expected to increase the polarity of the alkyl side chain, we favored this modification over additional perturbations to the steroid core, which we believed should serve as the major basis for recognition for a large fraction of cholesterol-binding proteins. The sterol probes, named *cis*-sterol, *trans*-sterol and *epi*-sterol, differ in the diastereomeric relationship between the C3-alcohol and C5-hydrogen groups appended to the cholesterol core, and we synthesized them from a common precursor, the bile acid hyodeoxycholic acid (**Supplementary Note**).

We obtained X-ray structures of the keto-acid intermediates corresponding to each cholesterol probe to verify their relative and absolute stereochemistry (**Fig. 1b**). As compared to the three-dimensional structure of cholesterol (extracted from a structure[24] in complex with NPC1; **Fig. 1b**), the *trans*-sterol probe exhibited the most similarity to cholesterol in terms of stereochemistry and molecular topology. Owing to its 3α-OH stereochemistry, the *epi*-sterol probe instead most resembled epicholesterol. Although the *cis*-sterol probe appeared bent in the crystal structure (**Fig. 1b**), it is probably the most flexible of the probes because of its structurally distinct *cis*-decalin–type A-B ring fusion[25]. This ring fusion stereochemistry, along with its 3α-OH stereochemistry, likely allows for the *cis*-sterol probe to adopt bent cholesterol-like conformations in solution that retain the equatorial orientation of the C3 hydroxyl group.

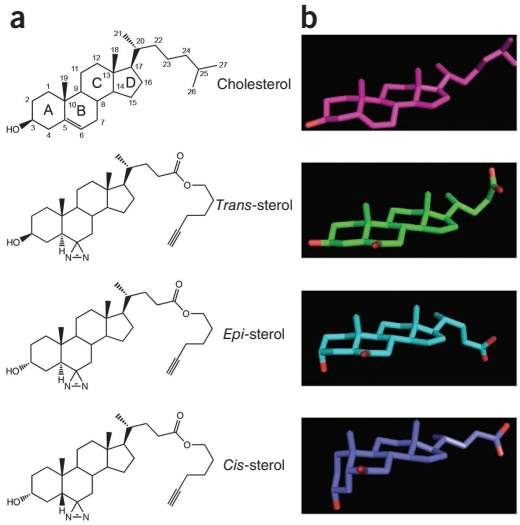

Figure 1 | Clickable photoreactive sterol probes. (**a**) Structures of cholesterol and three diastereomeric sterol chemoproteomic probes. Standard numbering and ring designations (A, B, C and D) are shown for cholesterol. (**b**) Three-dimensional structures of cholesterol and sterol probes as determined by X-ray crystallography; cholesterol structure is derived from Protein Data Bank (PDB) 3GKI (ref. 24).

Gel profiling of sterol-binding proteins in human cells

We first assessed sterol probe labeling of cellular proteins using SDS-PAGE analysis (**Fig. 2a** and Online Methods). Probe labeling for virtually all detected proteins was UV irradiation–dependent (**Fig. 2b**), indicating that these interactions reflect noncovalent binding events (versus the post-translational modification of proteins by cholesterol, as has been reported in select instances[15]). We observed concentration-dependent increases in protein labeling for all three probes (1–20 μM probe), with the *cis*-sterol and *trans*-sterol probes showing stronger overall protein-labeling profiles compared to the *epi*-sterol probe (**Fig. 2c**). In subsequent experiments we used conditions that produced substantial but submaximal labeling (10 μM probe).

We found that the protein-labeling profiles for all three sterol probes were competed to variable degrees by excess cholesterol (1×, 5× or 10× cholesterol supplemented as a methyl-β-cyclodextrin (mβCD) complex to enhance water solubility), with the *cis*-sterol probe showing the greatest sensitivity (**Fig. 2d**). Steroids or sterols with structures similar to that of cholesterol also blocked many of the protein-labeling events observed for the *trans*-sterol probe, whereas structurally less-related steroids exhibited little or no competition (**Supplementary Fig. 1**).

Mass spectrometry profiling of sterol-binding proteins

We aimed to characterize sterol-binding proteins, using methods based on biotin-streptavidin affinity coupled with stable-isotope labeling by amino acids in cell culture (SILAC) mass spectrometry[26], so that we could distinguish with precision proteins that specifically interact with sterol probes and assess the sensitivity of these interactions to competition by excess cholesterol (**Fig. 3a**). For our initial analyses, we treated heavy isotope–labeled ('heavy') HeLa cells with the *trans*-sterol probe (20 μM) for 30 min and irradiated the cells with UV light (5 min), whereas light isotope–labeled ('light') cells received either no probe treatment before exposure to UV light (vehicle control) or received the *trans*-sterol probe (20 μM) but were not irradiated (no–UV light control). We collected the cells, mixed their heavy and light proteomes 1:1, conjugated probe-labeled proteins to an azide-biotin tag by CuAAC and enriched these proteins using streptavidin chromatography. Then we digested the enriched proteins on-bead with trypsin and analyzed the resulting tryptic peptide mixture by liquid chromatography–mass spectrometry (Online Methods). Proteins that exhibited heavy:light SILAC ratios ≥ 5 for *trans*-sterol probe versus both vehicle and no–UV light control reactions were designated as 'sterol-interacting proteins'. About 850 proteins met these criteria (**Fig. 3b** and **Supplementary Tables 1** and **2**).

We next compared the proteome-labeling profiles of the *trans*-sterol probe with the *cis* and *epi*-sterol probes by SILAC. The mean labeling intensity ratio for probe-enriched proteins in the *trans*-sterol probe versus *cis*-sterol probe comparison was 0.9 (s.d. = 0.57; **Supplementary Fig. 2**), indicating that the *trans* and *cis*-sterol probes display similar protein-interaction profiles in cells. In contrast, for the *trans* versus *epi*-sterol

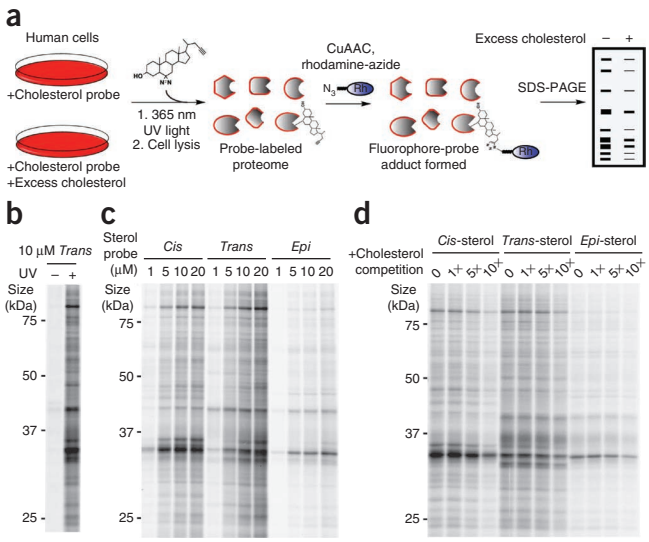

Figure 2 | Gel-based profiling of sterol-binding proteins in HeLa cells. (**a**) Scheme for treatment of live cells with sterol probes and competitive treatments. (**b**) SDS-PAGE analysis of HeLa cells treated with 10 μM *trans*-sterol probe, with and without 365-nm UV irradiation before click chemistry. (**c**) Concentration-dependent labeling of live HeLa cells with each probe at indicated concentrations. (**d**) Competition of sterol probe labeling profiles (10 μM probes) with cholesterol at 0 μM, 10 μM (1×), 50 μM (5×) and 100 μM (10×).

probe comparison, the mean ratio (2.1) as well as the standard deviation (1.2) were much higher (**Supplementary Fig. 2**), suggesting that the stereochemistry of the sterol hydroxyl group impacts probe-protein interactions in a variable manner.

Nearly 700 of the identified sterol-binding proteins showed strong selectivity (≥ threefold higher signals) for the *trans*-sterol probe over a nonsteroidal neutral lipid probe containing a diazirine and alkyne group embedded in an *N*-palmitoylethanolamine structure (*N*-palmitoylethanolamine-diazirine-alkyne (PEA-DA; **Supplementary Note**)) (**Fig. 3c** and **Supplementary Table 1**). Only 18 proteins from the sterol-binding group showed the opposite profile, exhibiting greater labeling with the PEA-DA probe (heavy/light signal ratio < 1.0; **Fig. 3c**).

Next we performed competitive profiling experiments, evaluating the *trans*-sterol probe for protein labeling in cells treated with excess cholesterol. We treated light and heavy HeLa cells with the *trans*-sterol probe (10 μM) in the presence or absence of 10× (100 μM) cholesterol, respectively. Approximately 300 proteins showed at least a 50% decrease in *trans*-sterol probe labeling intensity in cells treated with excess cholesterol (**Fig. 3d** and **Supplementary Table 3**). Over 250 of these cholesterol-sensitive targets also showed selective labeling by the *trans*-sterol probe compared to the PEA-DA probe (**Supplementary Table 1**), and the majority (>60%) of the competed proteins also showed evidence of cholesterol competition in experiments performed with the *cis*-sterol probe (**Supplementary Fig. 3**). We also performed parallel DNA microarray experiments and found that cholesterol-sensitive proteins, in general, exhibited no evidence of gene expression changes at the 30 min time point of competitive analysis (**Supplementary Fig. 4** and **Supplementary Table 4**).

Finally, as a control for incorporation of the heavy amino acids in our SILAC experiments, we treated heavy and light HeLa cells each with 20 μM *trans*-sterol probe, and combined and processed their proteomes as described above. The overall median and mean SILAC ratio for proteins detected in this experiment was 1.0 (**Supplementary Table 3**), indicative of > 95% heavy amino acid incorporation, and therefore ratios from other SILAC studies are presented without any correction factors.

Together, these quantitative mass spectrometry experiments enabled us to distribute the proteins that interacted with the *trans*-sterol probe into four groups: group I, which were both sensitive to cholesterol competition and selective for the *trans*-sterol probe over the PEA-DA probe (265 proteins); group II, which were sensitive but not selective (34 proteins), group III, which were selective but not sensitive (411 proteins), and group IV, which were neither sensitive nor selective (140 proteins) (**Fig. 3e** and **Supplementary Table 1**).

Analysis of group I cholesterol-binding proteins

Our detailed analysis of 265 group I proteins included both computational and experimental inquiries. We first noted that group I contains many proteins that are known to bind to cholesterol. These include Scap[12], caveolin (CAV1)[16], tetraspanin CD82 (ref. 20), the sterol transport protein ARV1 (ref. 27) and the sterol biosynthetic enzyme HMG-CoA reductase[17], which is known to be regulated by cholesterol through allosteric binding[17,18] (**Supplementary Table 5**). We found that the *trans*-sterol probe interacted with many other enzymes in the sterol biosynthetic pathway (**Fig. 3f,g**). FDFT1 and SQLE, two upstream enzymes in the sterol biosynthetic pathway that do not directly handle sterols as substrates or products were identified in group I (**Fig. 3g**), indicating that they may, like HMG-CoA reductase, interact with cholesterol through an allosteric mechanism. Groups II–IV also contained additional proteins known to interact with cholesterol, including, for instance, the lysosomal sterol transporter NPC1 (ref. 24) (**Supplementary Table 5**).

A broader survey of group I revealed that it contains representatives from virtually all major classes of proteins, including G protein–coupled receptors (a class of receptors that have been proposed to bind cholesterol to stabilize certain functional conformations[28]), ion channels, transporters and enzymes (**Fig. 4a**). Automated Kyoto Encyclopedia of Genes and Genomes (KEGG) pathway and Database for Annotation, Visualization and Integrated Discovery (DAVID) analysis tools[29,30] identified several types of proteins that were enriched in group I beyond the aforementioned sterol biosynthetic enzymes, including glycerophospholipid metabolic enzymes, protein glycosylation and degradation pathways, and protein networks that regulate membrane structure and dynamics (**Fig. 3f**). When considered in relation to human disease by analysis with the Online Mendelian Inheritance in Man (OMIM) database, group I was most highly enriched in proteins linked to neurological disorders as well as cardiovascular and metabolic diseases (**Fig. 4b**). Group I also contained a substantial number of proteins of uncharacterized function (**Fig. 4a**), including several that cluster into sequence-related sub-families (such as YIF1A/YIF1B, FNDC3A/FNDC3B, UNC84A/UNC84B, DPY19L1/DPY19L4, FAM114A1/FAM114A2 and FAM134A/FAM134B/FAM134C; **Supplementary Table 1**).

Evaluation of the subcellular distribution of group I proteins revealed, perhaps not surprisingly, that the vast majority (87%) are known or predicted integral membrane proteins (**Fig. 4c**).

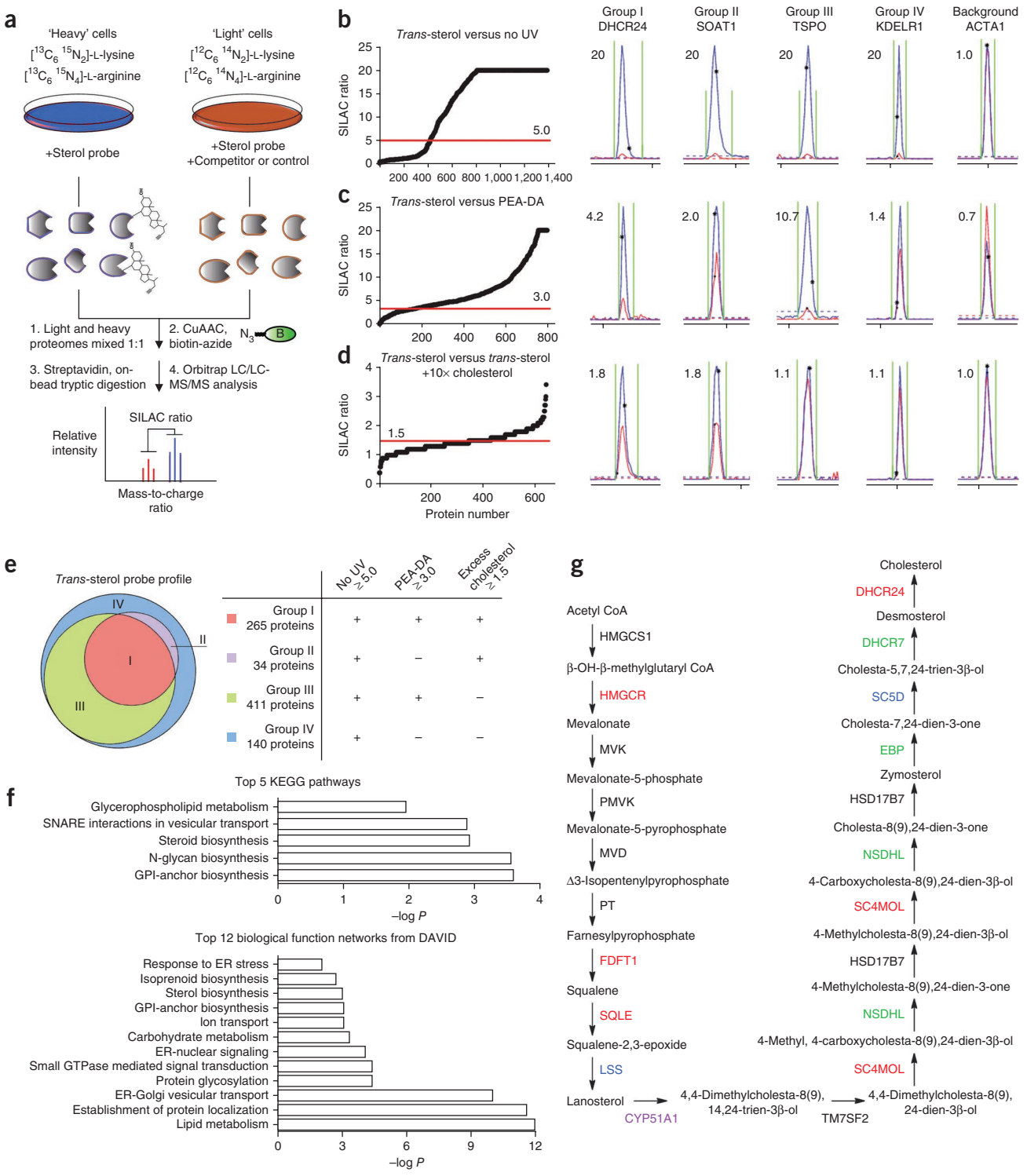

Figure 3 | Mass spectrometry–based profiling of sterol-binding proteins in HeLa cells. (**a**) Scheme for enrichment and analysis of sterol probe labeling profiles in mammalian cells by biotin-streptavidin methods and SILAC mass spectrometry analysis. (**b–d**) Heavy/light SILAC ratio plots (left; data in black) for total proteins identified in experiments in which we compared labeling profiles of the *trans*-sterol probe versus no-UV light control (**b**; 20 μM *trans*-sterol probe over 20 μM *trans*-sterol probe with no UV irradiation), the PEA-DA probe (**c**; 20 μM *trans*-sterol probe over 20 μM PEA-DA probe), and 10× cholesterol competition (**d**; 10 μM *trans*-sterol probe over 10 μM *trans*-sterol probe + 100 μM cholesterol). Red lines indicate threshold ratio values. Representative parent-ion mass (MS1) traces from each SILAC experiment (right) with calculated ratios indicated in the plots (ratios of ≥20 are listed as 20) for sterol-interacting proteins that fall into groups I–IV and for a nonspecific background protein. Blue traces denote the heavy (10 μM or 20 μM *trans*-sterol) trace; red traces denote the light (control or competed) trace; green lines designate the integration range for each peak quantification. (**e**) Distribution of group I–IV proteins for the *trans*-sterol probe labeling profile, with a summary of each group's threshold SILAC ratio requirements across each experiment. (**f**) Top 5 pathways determined by searching group I proteins in the KEGG database, and top 12 biological function networks determined by searching group I proteins in the DAVID gene ontology server. (**g**) *Trans*-sterol probe labeling profile for the cholesterol biosynthetic pathway, with colors (as in **e**) reflecting each enzyme's group designation (black, not detected).

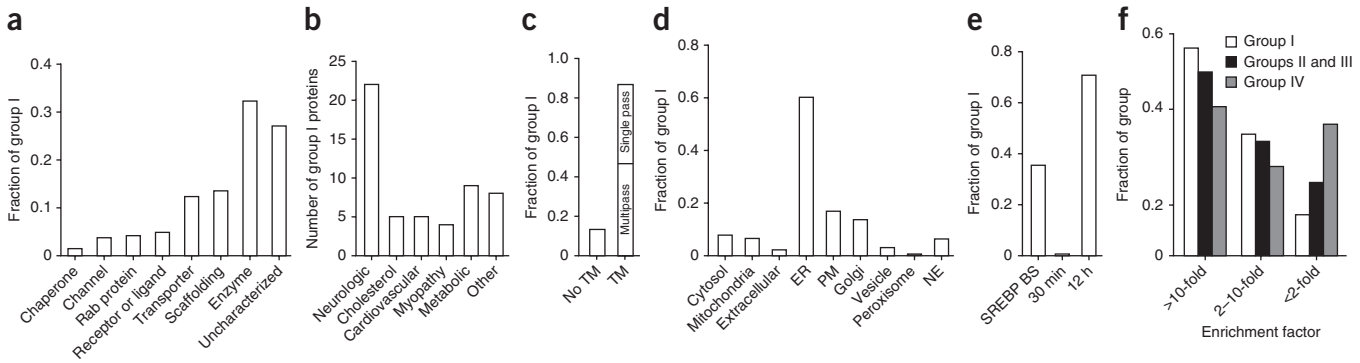

Figure 4 | Analysis of group I proteins. (**a**) Biochemical functions of group I proteins. (**b**) Group I proteins known to be genetically associated with human disease based on the OMIM database; the 'cholesterol' group represents diseases from all other groups that are known to manifest via aberrant cholesterol homeostasis. (**c**) Fraction of group I proteins that have known or predicted transmembrane (TM) domains. TM proteins are divided into single-pass versus multipass TM proteins. (**d**) Known or predicted subcellular localization of group I proteins. NE, nuclear envelope. Subcellular localization predictions were made by examining protein sequences using the PSORT II algorithm (http://psort.hgc.jp/form2.html). (**e**) Cholesterol regulation of group I proteins at the mRNA level. 'SREBP BS' denotes the fraction of group I proteins with SREBP transcription factor binding sites in the gene/promoter regions based on the Qiagen SABiosciences transcription factor database (http://www.sabiosciences.com/chipqpcrsearch.php?app=TFBS). The '30 min' and '12 h' labels denote the fraction of group I proteins with substantial (≥twofold) changes in mRNA levels after 100 μM cholesterol treatment for the indicated duration. (**f**) Enrichment (<2-fold, 2–10 fold and >10-fold) of group I, group II and III, and group IV proteins in *trans*-sterol probe data sets compared to their abundance in unenriched membranes.

These proteins were near-equally distributed between single-pass and multipass transmembrane proteins (**Fig. 4c**), and were dispersed across all subcellular membrane compartments with a notable enrichment in known or predicted endoplasmic reticulum (ER) proteins (**Fig. 4d**). Even though only 13% of proteins in group I were soluble proteins, the composition of this subset of proteins is intriguing: they include three kinases (HK1, HK2 and ADPGK) that convert glucose to glucose-6-phosphate, a key metabolic substrate for glycolysis and the pentose phosphate pathway. Both HK1 and HK2 are known to associate with cholesterol-rich regions of the mitochondria, although historically this interaction has been suggested to occur indirectly through binding VDAC channels[31]. Our chemoproteomic data indicate that HK1 and HK2 may also interact directly with cholesterol to facilitate their binding to mitochondria.

Cholesterol is known to regulate the expression of a large and diverse set of genes primarily through the Scap/SREBP system[12,14]. As noted above, very few of the group I proteins exhibited evidence of gene expression changes at the 30 min time point of our chemoproteomic analyses. About 35% of the group I proteins, however, have predicted SREBP transcription factor–binding sites in the promoter regions of their genes, and we determined that ~70% of these proteins exhibited at least a 100% increase or 50% decrease in their corresponding mRNA amounts 12 h after treatment of HeLa cells with cholesterol (100 μM) (**Fig. 4e**, **Supplementary Fig. 4**, **Supplementary Tables 1** and **4**). These data suggest that many proteins may be regulated by cholesterol at both the transcriptional (gene expression) and post-transcriptional (direct binding) levels.

We finally evaluated the extent to which our chemoproteomic method facilitated the enrichment and detection of sterol-binding proteins compared to analyses performed in unenriched proteomes. Group I proteins showed an average of 11 and 80 spectral counts in unenriched and probe-enriched proteomes, respectively, equating to an average enrichment factor of 7.3 (**Supplementary Table 6**). Additionally, more than 50% of group I proteins were enriched more than tenfold (and conversely fewer than 10% of these proteins were enriched less than twofold) in the *trans*-sterol probe data sets (**Fig. 4f**). We also observed no positive correlation between a protein's absolute spectral count values in the unenriched versus *trans*-sterol probe–enriched samples (**Supplementary Fig. 5**), indicating that group I proteins were not biased toward abundant integral membrane proteins.

Experimentally validating cholesterol-protein interactions

To validate seven representative group I proteins, including six previously unidentified sterol-binding proteins, we recombinantly expressed the proteins in HeLa cells and treated these cells with the *trans*-sterol probe, followed by CuAAC coupling to an azide-rhodamine tag, separation of proteins by SDS-PAGE and detection of probe-labeled proteins by in-gel fluorescence scanning (**Supplementary Fig. 6**). We also confirmed that these sterol-protein interactions were competitively inhibited by excess cholesterol without alterations in expression of the recombinant proteins (**Supplementary Figs. 6** and **7**).

DISCUSSION

Our strategy to map sterol-binding proteins on a global scale operates in living cells, which is important, given that the transport of cholesterol to discrete subcellular compartments and membrane microdomains is controlled by complex transport machinery[1]. This work thus builds on and extends previous efforts that used radioactive, photo-cross-linking probes[19,20] by providing a means to not only detect but also affinity-enrich and identify sterol-binding proteins from mammalian cells.

We should also mention some potential limitations of our approach and ways to address these shortcomings in the future. First, our initial set of probes may not detect certain sterol-protein interactions that are impaired by the diazirine and/or esterified alkyne modifications to the structure of cholesterol. The ester linkage might also be susceptible to cleavage by endogenous esterases, which could reduce the sensitivity of our proteomic profiles. These problems could be addressed by creating probes

in which the diazirine is moved to other locations on the sterol backbone and the esterified alkyne is replaced by distinct linkage chemistries. It might also be valuable to tailor probes to target proteins that bind to specific subsets of sterols (oxysterols[2], bile acids[4], steroids and others) as well as to perform competitive profiling where sterol analogs or other small molecules are tested for their ability to block specific sterol-protein interactions. We furthermore do not yet understand how, in most instances, sterol probes bind to their target proteins: developing a method to map the precise sites of sterol cross-linking to proteins would be valuable, and we note that the ester modification in our probe structures could provide a means to selectively release (through base hydrolysis) sterol-modified peptides from affinity-enrichment matrices. It would also be interesting to extend our analysis to other cell types and conditions (such as cells treated with statins or other cholesterol-lowering reagents), which could identify additional sterol-interacting proteins. Finally, we focused most of our attention in this study on group I proteins because they exhibited evidence of both selective binding to sterols over other lipids and sensitivity to cholesterol competition; however, groups II–IV also contain proteins known to interact with cholesterol. We do not know why cholesterol did not compete *trans*-sterol probe labeling of known sterol-binding proteins such as NPC1, but we observed competition for NPC1 with the *cis*-sterol probe (competition ratio = 2.1). Such probe-dependent variations in cholesterol competition could reflect differences in the local concentration of individual probes and/or cholesterol in specific organelles such as the lysosome or they may reflect differences in protein affinities for probes versus cholesterol. Regardless, that we found bona fide cholesterol-interacting proteins in groups I, II and III underscores the importance of considering the potential biological relevance for the entire >800 sterol-protein interactions reported here.

METHODS

Methods and any associated references are available in the online version of the paper.

Note: Supplementary information is available in the online version of the paper.

ACKNOWLEDGMENTS

We thank P. Baran for helpful advice on the synthesis of sterol probes, and A. Rheingold and C. Moore for X-ray crystallographic analysis. This work was supported by US National Institutes of Health (CA132630) and the Skaggs Institute for Chemical Biology.

AUTHOR CONTRIBUTIONS

J.J.H., S.E.T., M.J.N. and B.F.C. designed experiments; J.J.H., A.B.C. and S.E.T. performed experiments; J.J.H. and B.F.C. analyzed data; J.J.H. and B.F.C. wrote the manuscript.

COMPETING FINANCIAL INTERESTS

The authors declare no competing financial interests.

Published online at http://www.nature.com/doifinder/10.1038/nmeth.2368.
Reprints and permissions information is available online at http://www.nature.com/reprints/index.html.

1. Schroeder, F. *et al.* Caveolin, sterol carrier protein-2, membrane cholesterol-rich microdomains and intracellular cholesterol trafficking. *Subcell. Biochem.* **51**, 279–318 (2010).
2. Russell, D.W. Oxysterol biosynthetic enzymes. *Biochim. Biophys. Acta* **1529**, 126–135 (2000).
3. McLean, K.J., Hans, M. & Munro, A.W. Cholesterol, an essential molecule: diverse roles involving cytochrome P450 enzymes. *Biochem. Soc. Trans.* **40**, 587–593 (2012).
4. Russell, D.W. Fifty years of advances in bile acid synthesis and metabolism. *J. Lipid Res.* **50** (suppl.), S120–S125 (2009).
5. Badimon, L. & Vilahur, G. LDL-cholesterol versus HDL-cholesterol in the atherosclerotic plaque: inflammatory resolution versus thrombotic chaos. *Ann. NY Acad. Sci.* **1254**, 18–32 (2012).
6. Mirza, R. *et al.* DHCR24 gene knockout mice demonstrate lethal dermopathy with differentiation and maturation defects in the epidermis. *J. Invest. Dermatol.* **126**, 638–647 (2006).
7. Porter, F.D. Human malformation syndromes due to inborn errors of cholesterol synthesis. *Curr. Opin. Pediatr.* **15**, 607–613 (2003).
8. Herman, G.E. Disorders of cholesterol biosynthesis: prototypic metabolic malformation syndromes. *Hum. Mol. Genet.* **12** Spec No 1, R75–R88 (2003).
9. Cianciola, N.L., Carlin, C.R. & Kelley, T.J. Molecular pathways for intracellular cholesterol accumulation: common pathogenic mechanisms in Niemann-Pick disease Type C and cystic fibrosis. *Arch. Biochem. Biophys.* **515**, 54–63 (2011).
10. Rosenbaum, A.I. & Maxfield, F.R. Niemann-Pick type C disease: molecular mechanisms and potential therapeutic approaches. *J. Neurochem.* **116**, 789–795 (2011).
11. Weinhofer, I., Forss-Petter, S., Kunze, M., Zigman, M. & Berger, J. X-linked adrenoleukodystrophy mice demonstrate abnormalities in cholesterol metabolism. *FEBS Lett.* **579**, 5512–5516 (2005).
12. Brown, M.S. & Goldstein, J.L. The SREBP pathway: regulation of cholesterol metabolism by proteolysis of a membrane-bound transcription factor. *Cell* **89**, 331–340 (1997).
13. Gill, S., Chow, R. & Brown, A.J. Sterol regulators of cholesterol homeostasis and beyond: the oxysterol hypothesis revisited and revised. *Prog. Lipid Res.* **47**, 391–404 (2008).
14. Jeon, T.I. & Osborne, T.F. SREBPs: metabolic integrators in physiology and metabolism. *Trends Endocrinol. Metab.* **23**, 65–72 (2012).
15. Heal, W.P., Jovanovic, B., Bessin, S., Wright, M.H., Magee, A.I. & Tate, E.W. Bioorthogonal chemical tagging of protein cholesterylation in living cells. *Chem. Commun. (Camb.)* **47**, 4081–4083 (2011).
16. Hoop, C.L., Sivanandam, V.N., Kodali, R., Srnec, M.N. & van der Wel, P.C. Structural characterization of the caveolin scaffolding domain in association with cholesterol-rich membranes. *Biochemistry* **51**, 90–99 (2012).
17. Theesfeld, C.L., Pourmand, D., Davis, T., Garza, R.M. & Hampton, R.Y. The sterol-sensing domain (SSD) directly mediates signal-regulated endoplasmic reticulum-associated degradation (ERAD) of 3-hydroxy-3-methylglutaryl (HMG)-CoA reductase isozyme Hmg2. *J. Biol. Chem.* **286**, 26298–26307 (2011).
18. Motamed, M. *et al.* Identification of luminal Loop 1 of Scap protein as the sterol sensor that maintains cholesterol homeostasis. *J. Biol. Chem.* **286**, 18002–18012 (2011).
19. Thiele, C., Hannah, M.J., Fahrenholz, F. & Huttner, W.B. Cholesterol binds to synaptophysin and is required for biogenesis of synaptic vesicles. *Nat. Cell Biol.* **2**, 42–49 (2000).
20. Charrin, S. *et al.* A physical and functional link between cholesterol and tetraspanins. *Eur. J. Immunol.* **33**, 2479–2489 (2003).
21. Rostovtsev, V.V., Green, J.G., Fokin, V.V. & Sharpless, K.B. A stepwise Huisgen cycloaddition process: copper(I)-catalyzed regioselective "ligation" of azides and terminal alkynes. *Angew. Chem. Int. Edn. Engl.* **41**, 2596–2599 (2002).
22. Speers, A.E. & Cravatt, B.F. Profiling enzyme activities in vivo using click chemistry methods. *Chem. Biol.* **11**, 535–546 (2004).
23. Mintzer, E.A., Waarts, B.L., Wilschut, J. & Bittman, R. Behavior of a photoactivatable analog of cholesterol, 6-photocholesterol, in model membranes. *FEBS Lett.* **510**, 181–184 (2002).
24. Kwon, H.J. *et al.* Structure of N-terminal domain of NPC1 reveals distinct subdomains for binding and transfer of cholesterol. *Cell* **137**, 1213–1224 (2009).
25. Roberts, J.D. & Caserio, M. *Basic Principles of Organic Chemistry* 445–487 (Addison-Wesley, 1977).
26. Ong, S.E., Foster, L.J. & Mann, M. Mass spectrometric-based approaches in quantitative proteomics. *Methods* **29**, 124–130 (2003).
27. Tong, F. *et al.* Decreased expression of ARV1 results in cholesterol retention in the endoplasmic reticulum and abnormal bile acid metabolism. *J. Biol. Chem.* **285**, 33632–33641 (2010).
28. Thompson, A.A. *et al.* GPCR stabilization using the bicelle-like architecture of mixed sterol-detergent micelles. *Methods* **55**, 310–317 (2011).
29. Huang da, W., Sherman, B.T. & Lempicki, R.A. Systematic and integrative analysis of large gene lists using DAVID bioinformatics resources. *Nat. Protoc.* **4**, 44–57 (2009).
30. Huang da, W., Sherman, B.T. & Lempicki, R.A. Bioinformatics enrichment tools: paths toward the comprehensive functional analysis of large gene lists. *Nucleic Acids Res.* **37**, 1–13 (2009).
31. Pastorino, J.G. & Hoek, J.B. Regulation of hexokinase binding to VDAC. *J. Bioenerg. Biomembr.* **40**, 171–182 (2008).

ONLINE METHODS

Chemical probe synthesis. See **Supplementary Note**.

Cell culture and live cell labeling. HeLa cells were grown at 37 °C under a humidified 5% CO_2 atmostphere, in a culture medium consisting of high-glucose DMEM (HyClone) supplemented with 10% FBS (Gemini), and penicillin, streptomycin and glutamine (PSQ; Cellgro). For SILAC experiments, the culture medium was replaced with SILAC DMEM (Thermo) supplemented instead with 10% dialyzed FBS, PSQ and 100 μg/ml [$^{13}C_6$,$^{15}N_4$]L-arginine-HCl and [$^{13}C_6$,$^{15}N_2$]L-lysine-HCl (Sigma-Aldrich). Cells were passaged at least six times in isotope-containing medium before being used for analysis by liquid chromatography–tandem mass spectrometry (LC-MS/MS).

To facilitate delivery to cells, all sterols and steroids, including the sterol probes, were complexed in aqueous solution to mβCD (Sigma-Aldrich) for at least 12 h before dilution in culture medium for labeling at working concentrations indicated in the main text, adapted from published procedures[32]. The desired amount of sterol or steroid was added to a saturated aqueous mβCD (38 mM) solution to generate a concentrated stock, and the mixture was agitated at room temperature overnight; solutions were filtered before use the following day. Aqueous stock solutions of the *trans*-sterol probe were prepared at 2 mM; the *cis*-sterol and *epi*-sterol probes were prepared at 1.2 mM; cholesterol and other sterols for competition were prepared at 4 mM; steroids were prepared at 5 mM. Nonsteroidal lipids, C_{17}-MAGE and di-C_{15}-DAG, as well as the PEA-DA probe were suspended in DMSO (10 mM) and diluted to working concentrations directly in culture medium.

Before live-cell labeling, aqueous stock solutions of each sterol probe or competitor (or DMSO stock solution of lipids) were combined in opaque centrifuge tubes and then diluted to final working concentrations in culture medium under dim ambient light. Unmodified culture medium was then removed from the cells and replaced with probe-containing medium. Cells were then incubated at 37 °C for 30 min in the dark to load the cells with sterol probe and competitors. After this time, cells were washed quickly with cold PBS and then irradiated for 5 min in cold PBS under 365-nm UV light in a FB-UVXL-1000 UV cross-linker (Fisher). Cells were then collected by scraping, and the cell pellet was frozen at −80 °C until processing for gel or LC-MS/MS analysis.

Sample processing for analysis by SDS-PAGE or LC-MS/MS. Frozen cell pellets were thawed on ice and lysed in PBS by sonication. Protein concentrations of cell lysates were determined using the BCA protein assay on a microplate reader. Click chemistry was then performed as previously described[33] directly in whole-cell lysates in PBS. For analysis by gel, 50 μg of protein was used, adjusted to a protein concentration of 1 mg/ml (50 μl), and mixed with 20 μM rhodamine-azide, 1 mM Tris(2-carboxyethyl)phosphine (TCEP, Sigma-Aldrich), 100 μM Tris[(1-benzyl-1H-1,2,3-triazol-4-yl)methyl]amine (TBTA) (Sigma-Aldrich) and 1 mM $CuSO_4$ in PBS at room temperature. After 1 h, samples were mixed with SDS sample loading buffer and loaded without boiling on a 10% SDS-PAGE gel, separated and imaged using a Hitachi FMBIO-II flatbed fluorescence scanner. Fluorescence images are shown in grayscale.

For proteomic analysis, 1 mg of both heavy and light lysates were mixed in a 1:1 ratio, and then combined with 500 μM biotin-azide, 100 μM TBTA, 1 mM TCEP and 1 mM $CuSO_4$ in 400 μl PBS for 1 h. Water (100 μl), methanol (500 μl) and chloroform (125 μl) were then added directly to the reaction mixture and mixed vigorously by vortexing. The biphasic solution was then centrifuged at 1,400*g* for 20 min at 4 °C, and protein was pelleted at the phase interface as a solid disk. Liquid layers were discarded, and the protein was washed by sonication in 1:1 methanol/chloroform (500 μl first wash, 250 μl second wash) followed by centrifugation at 16,000*g* for 10 min at 4 °C to repellet. The protein pellets were air-dried briefly, and then resuspended by sonication in 500 μl water containing 25 mM ammonium bicarbonate and 6 M urea. To this solution, 5 μl of a 1 M DTT solution in water was added, followed by 140 μl 10% SDS in water, and the solution was heated at 65 °C for 15 min. The samples were cooled briefly on ice, then 40 μl of a 0.5 M iodoacetamide (Sigma-Aldrich) solution in water was added, and the samples were incubated at room temperature for 30 min in the dark. The samples were then diluted to 6 ml with PBS, and enriched over streptavidin (Thermo; 100 μl slurry) for 2 h at room temperature. The beads were washed once with 10 ml 1% SDS in PBS, then three more times with 10 ml PBS. The beads were then transferred to a 1.5 ml screw-cap tube in 200 μl 25 mM ammonium bicarbonate with 2 M urea in water, with 1 mM calcium chloride and 2 μg sequencing-grade porcine trypsin (Promega) and then digested at 37 °C overnight. The digest supernatant was then collected by filtration of the resin, which was washed with 100 μl PBS. The combined filtrate and wash for each sample was then acidifed with 16 μl formic acid and then pressure-loaded onto a biphasic (strong cation exchange/reverse phase) capillary column for analysis by two-dimensional (2D) LC-MS/MS. Unenriched samples were processed in the same fashion, but the enrichment step was omitted and instead 200 μg of processed protein was committed to tryptic digestion and multidimensional protein identification technology (MudPIT) analysis.

Mass spectrometry and data processing. Mass spectrometry was performed using a Thermo Orbitrap Velos mass spectrometer. Peptides were eluted using a five-step multidimensional LC-MS (MudPIT[34]) protocol (using 0%, 25%, 50%, 80% and 100% salt bumps of 500 mM aqueous ammonium acetate, followed by an increasing gradient of aqueous acetonitrile and 0.1% formic acid in each step), and data were collected in data-dependent acquisition mode (two MS1 microscans (400–1800 mass to charge ratio (*m/z*)) and 30 data-dependent fragmentation (MS2) scans) with dynamic exclusion enabled (repeat count of 1, exclusion duration of 20 s) with monoisotopic precursor selection enabled. All other parameters were left at default values. Unenriched membrane preparations were eluted using the same chromatographic steps and instrument settings. SEQUEST[35] searches allowed for variable oxidation of methionine (+15.9949 *m/z*), static modification of cysteine residues (+57.0215 *m/z*; iodoacetamide alkylation) and no enzyme specificity. Each data set was independently searched with light and heavy parameter files; for the light search, all other amino acids were left at default masses; for the heavy search, static modifications on lysine (+8.0142 *m/z*) and arginine (+10.0082 *m/z*) were specified. The precursor-ion mass tolerance was set to 50 p.p.m. and the fragment-ion mass tolerance was the

default assignment of 0. The data were searched using a human reverse-concatenated nonredundant (gene-centric) FASTA database that combines International Protein Index (IPI) and Ensembl identifiers. The resulting matched MS2 spectra were assembled into protein identifications, then filtered using DTASelect (version 2.0.47), and only half-tryptic or fully tryptic peptides were accepted for identification, and only fully-tryptic peptides were considered for quantification. Peptides were restricted to a specified false positive rate of 1%. Redundant peptide identifications common between multiple proteins were allowed, but the database was restricted to a single consensus splice variant. SILAC ratios were quantified using in-house software as described (CIMAGE[36]). Briefly, extracted MS1 ion chromatograms (± 10 p.p.m.) from both 'light' and 'heavy' target peptide masses (*m/z*) were generated using a retention time window (± 10 min) centered on the time when the peptide ion was selected for MS/MS fragmentation, and subsequently identified. Next, the ratio of the peak areas under the light and heavy signals (signal-to-noise ratio > 2.5) are calculated. Computational filters used to ensure that the correct peak-pair is used for quantification include a co-elution correlation score filter ($R^2 \geq 0.8$), removing target peptides with bad co-elution profile, and an 'envelope correlation score' filter ($R^2 > 0.8$) that eliminates target peptides whose predicted pattern of the isotopic envelope distribution does not match the experimentally observed high-resolution MS1 spectrum. Also, peptides detected as singletons, where only the heavy or light isotopically labeled peptide was detected and sequenced, but which passed all other filtering parameters, were given a standard ratio of 20, which is the maximum SILAC ratio reported here. All reported SILAC experiments were run in duplicate, except the cholesterol competition experiment, which was run in quadruplicate.

After automated processing, data sets were filtered and analyzed manually based on more stringent and experiment-specific criteria. Only proteins that showed at least two unique identified and quantified peptides between four control runs (*trans*-sterol probe versus vehicle and versus 'no UV', each in duplicate), and that showed at least ratio of 5.0 when the heavy, *trans*-sterol probe–enriched signal was compared to the background signal, were considered for subsequent analysis by comparison to the PEA-DA labeling profile, and to cholesterol competition. Only proteins that showed at least a ratio of 3.0 when *trans*-sterol probe–labeled cells were compared to PEA-DA–labeled cells were considered 'selective' and could be considered group III or higher, and only proteins that showed at least a ratio of 1.5 when competed by 10× cholesterol and showed at least two quantified unique peptides across four competition runs were considered 'sensitive' for subsequent analysis and consideration as group II or higher. All experimental SILAC ratios presented are the mean of the median ratios of all quantified peptides for each protein from each replicate for each experiment.

Meta-analyses (**Fig. 4**) of the sensitive and selective group of *trans*-sterol probe targets were performed using several online resources and servers. Automated gene ontology and pathway enrichment analyses were performed by uploading the group I protein list to the DAVID bioinformatics website and performing enrichment analyses. Protein annotations in **Figure 4** were obtained from primary literature sources, http://genecards.com, the Qiagen SABiosciences transcription factor database and the OMIM database. Transmembrane domains were predicted, as necessary, by PSORT II and TMHMM prediction servers.

Microarray analysis of cholesterol-induced transcriptional changes. To verify that the observed cholesterol competition was most likely due to direct physical competition of probe binding and was not due to cholesterol-mediated expression changes for each sensitive target, we incubated HeLa cells with or without 20 μM *cis* probe and 100 μM cholesterol for 30 min and 12 h, then collected total cellular mRNA from each treatment using the Qiagen RNEasy kit, and submitted 8 μg total mRNA (combination of three biological replicates) per sample to the Scripps Research Institute DNA Array core facility, for quantitative transcriptomic analysis by microarray, using the HU133 Set GeneChip (Affymetrix) and the Affymetrix GeneChip Expression 3′ Amplification One-Cycle protocol.

Recombinant expression and validation cholesterol competition of targets. To validate protein-cholesterol interactions identified by the *trans*-sterol probe for which there was no previous evidence of cholesterol binding, cDNAs encoding SQLE, FDFT1, PGRMC1, POR, ADPGK, CYP20A1 and JAGN1 were obtained (OpenBiosystems), and these proteins were recombinantly overexpressed as the full-length, unmodified proteins (except JAGN1, which was expressed with a C-terminal myc-his epitope-tag) in HeLa cells via transfection with Fugene HD according to the manufacturer's protocol. Forty-eight hours after transfection, cells were labeled *in situ* with either 5 μM or 10 μM *trans*-sterol probe, with or without 10× (50 μM or 100 μM, respectively) cholesterol. Both the competed and non-competed transfected samples were compared to a control (**Supplementary Fig. 6**) transfected with a cDNA encoding a distinct protein, on a 10% SDS-PAGE gel, and equal expression of the protein of interest between competed and noncompeted samples was verified via western blot of the same samples on a gradient (4–20%) gel using commercial antibodies specific to each protein. Antibodies used in this study were: monoclonal mouse anti-myc (1:10,000; Invitrogen, 46-0603), polyclonal rabbit anti-POR (1:1000; Sigma-Aldrich, SAB1410996), polyclonal mouse anti-FDFT1 (1:1,000; Sigma-Aldrich, SAB1405805), monoclonal mouse anti-ADPGK (1:1,000; Sigma-Aldrich, WH0083440M1, clone 1E4), polyclonal rabbit anti-PGRMC1 (1:2,000; Sigma-Aldrich, HPA002877), polyclonal mouse anti-SQLE (1:1,000; Sigma-Aldrich, SAB1406474), monoclonal mouse anti-actin (1:2,000; Sigma-Aldrich, A3853, clone AC-40) and polyclonal rabbit anti-CYP20A1 (1:100; Thermo, PA5-14356).

32. Christian, A.E., Haynes, M.P., Phillips, M.C. & Rothblat, G.H. Use of cyclodextrins for manipulating cellular cholesterol content. *J. Lipid Res.* **38**, 2264–2272 (1997).
33. Martin, B.R., Wang, C., Adibekian, A., Tully, S.E. & Cravatt, B.F. Global profiling of dynamic protein palmitoylation. *Nat. Methods* **9**, 84–89 (2012).
34. Washburn, M.P., Wolters, D. & Yates, J.R. III. Large-scale analysis of the yeast proteome by multidimensional protein identification technology. *Nat. Biotechnol.* **19**, 242–247 (2001).
35. Eng, J., McCormack, A.L. & Yates, J.R. An approach to correlate MS/MS data to amino acid sequences in a protein database. *J. Am. Soc. Mass Spectrom.* **5**, 976–989 (1994).
36. Weerapana, E. *et al.* Quantitative reactivity profiling predicts functional cysteines in proteomes. *Nature* **468**, 790–795 (2010).

doi:10.1038/nmeth.2368